

Partitioned Active Learning for Heterogeneous Systems

Cheolhei Lee, Kaiwen Wang, Jianguo Wu, Wenjun Cai, and Xiaowei Yue

Abstract—Cost-effective and high-precision surrogate modeling is a cornerstone of automated industrial and engineering systems. Active learning coupled with Gaussian process (GP) surrogate modeling is an indispensable tool for demanding and complex systems, while the existence of heterogeneity in underlying systems may adversely affect the modeling process. In order to improve the learning efficiency under the regime, we propose the partitioned active learning strategy established upon partitioned GP (PGP) modeling. Our strategy seeks the most informative design point for PGP modeling systematically in two steps. The global searching scheme accelerates the exploration aspect of active learning by investigating the most uncertain design space, and the local searching exploits the active learning criterion induced by the local GP model. We also provide numerical remedies to alleviate the computational cost of active learning, thereby allowing the proposed method to incorporate a large amount of candidates. The proposed method is applied to numerical simulation and real world cases endowed with heterogeneities in which surrogate models are constructed to embed in (i) the cost-efficient automatic fuselage shape control system; and (ii) the optimal design system of tribocorrosion-resistant alloys. The results show that our approach outperforms benchmark methods.

Index Terms—Active learning, Sequential design, Gaussian process, Surrogate modeling

I. INTRODUCTION

GAUSSIAN process (GP) has been extensively utilized for predictive modeling of diverse industrial systems such as robotics, aerospace, and manufacturing process controls [1]–[3] due to the capability of nonlinear distance-based interpolation and uncertainty quantification [4]. Highly reliable GP models can serve as numerically fast and inexpensive surrogate models or optimization tools [5], and they are indispensable requisites for automation of demanding processes such as zero-defect manufacturing systems, digital twins, and complex process controls [6]–[8]. However, building such high-quality GP models can be very challenging in practice when target systems exhibit heterogeneity in design spaces, such as abrupt variations in gradient norms and frequencies, or discontinuity. Such heterogeneity is ubiquitous in industrial and engineering systems. For example, composite materials, one of the most versatile material in various contemporary products, are

anisotropic and highly nonlinear to external treatments [9], so they may have multiple patterns in the design space [2], [10].

The difficulties of GP modeling under the aforementioned circumstance lie in modeling and design of experiment (DOE) aspects. In the modeling perspective, stationary GPs cannot efficiently reflect different spatial characteristics of heterogeneous systems. Nonstationary kernels can be possible solutions, while they are more intractable in analysis and interpretation than stationary GPs. In terms of DOE, which is the main concern of this paper, the heterogeneity compels more judicious design strategies than nonsequential design such as factorial, Latin hypercube design (LHD) [11], and the traditional passive learning that relies on independent and identically distributed (i.i.d.) sampling. For example, Fig. 1 illustrates corrosive rates of alloys emulated with a finite element analysis (FEA) model over two pairs of control variables. We can find that the response surface includes three heterogeneous subregions. The property parameters are quite different between different subregions. Since the green region is less interesting than elsewhere, we can conjecture that it is inefficient to weigh equally over the entire region.

Partitioned GPs (PGPs) can overcome the limitation of stationary GPs for heterogeneous systems by allocating multiple independent local GPs on disjoint subregions. These subregions compose the entire design space. Subregions are defined or estimated according to distinguishable characteristics of target systems, so PGPs can accommodate different characteristics with local GPs. Moreover, the partitioning may improve the scalability of GPs, one of main drawbacks of them, by introducing sparsity in their covariance matrices. Due to these advantages, several approaches to realize PGPs have been proposed [12]–[16]. However, most of them basically are devised with nonsequential designs that are suboptimal in heterogeneous systems, since they do not consider outputs and characteristics of intermediate models that can be quite informative for understanding characteristics of the target system. Therefore, a smarter design strategy should be developed in order to achieve the sequential optimal design in heterogeneous systems.

Contrary to nonsequential designs, active learning sequentially selects design points in the modeling phase after observing intermediate models and outputs, thereby maximizing the information for modeling [17], [18]. Active learning is also called sequential design, adaptive sampling, or optimal design in different research fields, while they pursue the same objective, i.e., finding the best subset of inputs from the design space based on some information criteria. For a few decades, active learning coupled with GP modeling has been frequently

C. Lee and X. Yue are with the Grado Department of Industrial and Systems Engineering, Virginia Tech, Blacksburg, VA, 24061 USA (e-mail: cheolheil@vt.edu; xwy@vt.edu)

K. Wang and W. Cai are with the Department of Materials Science and Engineering, Virginia Tech, Blacksburg, VA, 24061 USA (e-mail: kaiwen-wang@vt.edu; caiw@vt.edu).

J. Wu is with the Department of Industrial Engineering and Management, Peking University, Beijing, 100080 China (e-mail: j.wu@pku.edu.cn)

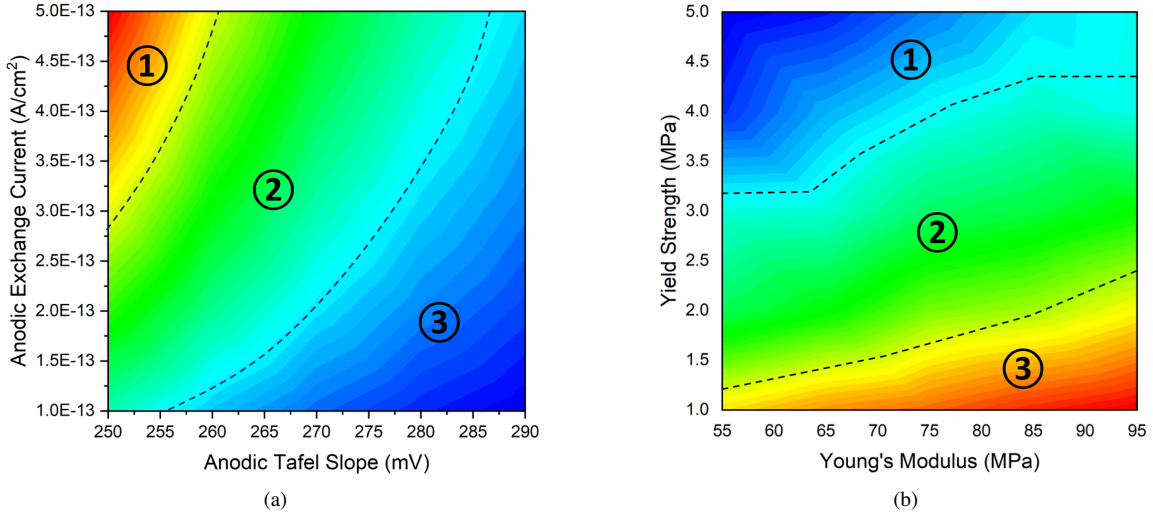


Fig. 1. Corrosive rate of alloys with different control variables. (a) Response surface with Tafel slope and anodic exchange current. (b) Response surface with Young's modulus and yield strength. Each partitioning (3 subregions) is given according to the gradient norm of response.

addressed in both methodological perspective and applications [19]–[22], and the approach has shown remarkable performance in practice. However, active learning itself has mostly been coupled with single GP (SGP), so the strategies may not work for the systems with heterogeneity, such as systems modeled by PGPs. More explicitly, the information criterion induced from a SGP can be inconsistent for multiple independent (or weakly correlated) subregions, as well as be computationally inefficient. Moreover, heterogeneity can mislead some active learning algorithm by taking into account local behavior of system that may hinder efficient learning of GP models.

Motivated from the aforementioned limitations of existing active learning strategies for PGPs, we propose a bespoke active learning strategies for PGP modeling of heterogeneous systems. We choose the most uncertain subregion in the design space in the first global searching step, and then the localized IMSE criterion is used to select the design point within the subregion. The contributions of this paper are summarized as follows. First, we develop an active learning criterion that is built upon the PGPs. Second, we propose a novel two-step searching scheme that exploits the partitioned structure of PGPs so as to improve the efficiency of modeling process for the heterogeneous systems. Third, we provide numerical remedies to reduce the computational cost of information criterion in our active learning algorithm.

The remainder of this paper is organized as follows. In Section II, we review existing active learning strategies for GPs and PGP modeling approaches. Section III describes our active learning algorithm for PGPs, and applicable techniques for improving the learning efficiency and numerical costs. In Section IV, we implement our method on partitioned GP modeling of two simulation functions in different dimensions, and predictive modeling of composite structure deformations and corrosive rates of alloys are considered in Section V to validate our method in real world applications. A brief summary of this paper is provided in Section VI.

II. LITERATURE REVIEW

In this section, we review related literature of existing active learning strategies for SGPs and recent applications in real world cases. Afterward, we discuss literature of PGP methodologies and some active learning schemes therein.

A. Active Learning for Gaussian Processes

Due to the capability of uncertainty quantification with GPs, the predictive uncertainty has been frequently involved in the construction of active learning criteria for GPs. Seo *et al.* [19] compared two criteria for GP regression. Both are suggested respectively by [23] and [24], so called by active learning Mackay (ALM) and active learning Cohn (ALC). The ALM refers to the variance-based criterion that selects unobserved points with the largest predictive uncertainty quantified with variance or standard deviation. A number of applications exist that employ the ALM due to its simplicity and straightforwardness [25]. Meanwhile, the ALC refers to the integrated mean squared prediction error (IMSE) that seeks a point expected to reduce the most the integrated variance of the GP model over the design space, and it has been also widely applied to different GP frameworks. Chen *et al.* [26] utilized the IMSE criterion for stochastic kriging [27], so as to balance between exploration over the design space and exploitation with additional replications. Yue *et al.* [22] also proposed two active learning algorithms for GP surrogate models of multimodal systems. The variance-based weighted active learning (VWAL) uses the weighted sum of variance-based criteria of modes, and the D-optimal weighted active learning (DOWAL) uses the fisher information matrix with the same weighting procedure of VWAL. The Bayesian optimization (BO) [28] is another interesting trend of sequential sampling that also utilizes the predictive uncertainty of GPs for global optimization problems. There are several criteria (also called by acquisition functions) for the BO such as the expected improvement (EI) and the probability of improvement (PI).

They refer to the GP surrogate model of blackbox objective function, thereby choosing a point to be queried most likely to be optimal. However, it is noteworthy that both the BO and the active learning for surrogate modeling pursue reduction in sampling cost, while they have different purposes: finding the optimal solution of blackbox function, and minimizing the predictive error of surrogate model over the entire design space.

For strategies that do not take the predictive uncertainty into account or less consider, Pasolli *et al.* [29] suggested to use space-filling designs in the Kernel Hilbert space induced by intermediate GP models. Freytag *et al.* [30] and Kading *et al.* [31] used expected model output change as their criterion for active learning. The strategy chooses the location where is expected to induce the largest change of model outputs over the design space. Erickson *et al.* [32] and Marmin *et al.* [21] involve the gradient of GP model's response in active learning so as to draw more samples from where the response abruptly changes. Consequently, the gradient-based criterion focuses more on local variation than the entire design space, thereby reducing the prediction error more efficiently. Uteva *et al.* [25], [33] referred to the discrepancy of multiple GP models trained on different subsets of data. However, aforementioned active learning strategies mostly support SGP models that are inappropriate for modeling of our targeting heterogeneous systems. Moreover, it is inefficient to directly apply them to PGPs, since they cannot consider the partitioned structure of PGP models. Liu *et al.* [18] provided a comprehensive active learning strategies for GP surrogate modeling of engineering systems.

B. Partitioned Gaussian Processes

Although there are techniques other than partitioning design spaces to overcome the limitation of stationary GP models such as input-dependent length scale, warping and convolution kernels [21], [34], [35], we mainly focus on PGPs that explicitly partitions design space for multiple GP models. Kim *et al.* [13] proposed the piecewise GP using Voronoi tessellation with training dataset for partitioning the design space. Advantages of Voronoi tessellation are simplicity, consistency, and distance-based algorithm that coincides with stationary GPs. They estimated the number of regions and centers with the Monte-Carlo approach, and fitted independent GP models for subregions. Subsequently, Pope *et al.* [16] generalized the partitioning by merging convex Voronoi cells in order to generate nonconvex subregions, and relaxed centers of cells. Gramacy *et al.* [14] proposed the Treed GP (TGP) using decision trees for partitioning. They fitted independent local GPs on each leaf corresponds to partitioned subregions. Heaton *et al.* [15] proposed to partition the design space prior to GP modeling by hierarchical clustering referring to finite differences of samples. They insist that the approach allows to avoid expensive Markov Chain Monte-Carlo (MCMC) algorithm of aforementioned approaches. The mixture of GP experts proposed by [12] is another approach using multiple stationary GPs. Although components in their modeling process have own terminologies, the underlying idea is very close to aforementioned methodologies.

To the best of our knowledge, there exist only a few strategies for PGPs. Pope *et al.* [16] proposed to an active learning algorithm with their PGP modeling that takes a point within regional boundaries that maximizes the space-filling property of design points. However, it focuses more on detecting discontinuity in design space rather than reducing the prediction error over the design space, although such discontinuity is rare in industrial and engineering applications. Gramacy *et al.* [20] and Konomi *et al.* [36] provided active learning algorithms that are modified versions of [19] for the TGP. They provided more elaborate techniques considering the posterior structure of partitioned design space. However, their approaches are highly dependent to the tree classifier, while the tree partitioning mostly induces boundaries parallel to axes that may not be realistic in practice [15], [16]. Moreover, the choice of design point candidates are dependent to the areas of partitioned regions, so it can be irrelevant when a plausible partition is not realizable with a few tree-partitioned regions. If we expand our field of interest to classification with generic machine learning models, Cortes *et al.* [37] has similar concept of ours in the macroscopic aspect, while there are main differences: (i) they consider classification problems, thus theoretical bounds they provided may be intractable in practice with regression problems (e.g., model capacity, bounded loss); and (ii) they consider the disagreement-based criterion within a model class, while we advocate the IMSE criterion, which belongs to variance reduction criterion [17].

III. PARTITIONED ACTIVE LEARNING

In this section, we propose our active learning algorithm for the PGP modeling. First, we briefly discuss a generic framework of PGPs as the initialization step of active learning, and elucidate our strategy consecutively. Lastly, applicable remedies are provided for the numerical improvement of algorithm.

A. Initialization with Partitioned Gaussian Processes

We aim to build a PGP model of a system which is expensive to operate. Suppose that the system can be expressed as a deterministic function f defined over a design space $\mathcal{X} \subset \mathbb{R}^d$ mapping to R , and the function is endowed with the heterogeneity in \mathcal{X} . Let $H : \mathcal{X} \rightarrow R$ be the PGP, our estimated model of f , and $g : \mathcal{X} \rightarrow \{1, \dots, M\}$ be a region classifier that partitions \mathcal{X} into M disjoint regions such that $\mathcal{X} = \bigcup_{m=1}^M X_{(m)}$ accordance with the heterogeneity. Then, the PGP composed of M local GPs is defined as

$$H(x) = \sum_{m=1}^M \mathbf{1}_{\{g(x)=m\}} h_{(m)}(x), \quad (1)$$

where $\mathbf{1}_{\{C\}}$ is an indicator function which has value 1 when C is true and 0 otherwise, and $h_{(m)}$ is a local GP assigned to the m -th subregion $X_{(m)}$. Although PGPs can take any valid kernel for their local GPs, we mainly consider stationary kernel family such as radial basis function (RBF) and Matérn. The local GP defined over $X_{(m)}$ with the RBF kernel is defined as

$$h_{(m)}(x) \sim \mathcal{GP} \left(\mu_{(m)}(x), \sigma_{(m)}^2(x, x') \right), \quad x, x' \in X_{(m)} \quad (2)$$

$$\begin{aligned}\sigma_{(m)}^2(x, x') &:= k_{(m)}(x, x') \\ &= c_{(m)}^2 \exp\left(-\frac{(x-x')^2}{l_{(m)}^2}\right) + \sigma_w^2 \mathbf{1}_{\{x=x'\}},\end{aligned}\quad (3)$$

where $\mu_{(m)}(x)$ is the mean function assumed to be 0 without loss of generality, and $k_{(m)}(x, x')$ is the kernel in which nonnegative $c_{(m)}^2$, $l_{(m)}^2$ and σ_w^2 are referred as scale, length and noise hyperparameters. We assume that σ_w^2 is shared with all subregions, so that the PGP H would have $2M + 1$ hyperparameters at least, for which we denote by $\Theta = \{\theta_{(1)}, \dots, \theta_{(M)}, \sigma_w^2\}$, $\theta_{(m)} = \{c_{(m)}^2, l_{(m)}^2\}$.

Suppose we have finite n observations on $X_n = \{x_1, \dots, x_n\} \subset \mathcal{X}$ such that $D_n = \{(x_1, y_1), \dots, (x_n, y_n)\}$, where $y_i = f(x_i) + \epsilon$ and $\epsilon \sim \mathcal{N}(0, \sigma_w^2)$. We use parentheses numbers in subscription of each sample to indicate the associated region as $x_{(m),i} \in X_{(m)}$, and subsequent normal numbers represent sample indices and associated number of samples. The PGP model can be optimized with D_n by maximizing the marginal likelihoods of local GPs, proportional to

$$\begin{aligned}\ell(\Theta) &\propto \prod_{m=1}^M \mathbf{y}_{(m)}^\top K_{(m)}^{-1}(\theta_{(m)}) \mathbf{y}_{(m)} \\ &\quad - \log \det K_{(m)}(\theta_{(m)}) - n_{(m)} \log 2\pi,\end{aligned}\quad (4)$$

where $\mathbf{y}_{(m)}$ is a vector comprised of observations on $X_{(m)}$, $k_{(m)}(\theta_{(m)})$ is the covariance matrix defined as $(k_{(m)})_{ij} = k_{(m)}(x_{(m),i}, x_{(m),j})$, and $n_{(m)}$ is the number of samples in m -th region. Note that the PGP's likelihood is the multiplication of that of local GPs due to their independence. Consequently, possibly with some ordering process, the PGP produces a block diagonal covariance matrix which implies that the numerical advantage of PGPs comes from the sparsity. Although the construction of entire covariance matrix is generally unnecessary in practice, it informs us that the model can be manipulated more efficiently by treating each local GP independently.

The performance of PGP is determined by credibility of the region classifier g and estimated hyperparameters of local GPs Θ . When the underlying partitioning rule is unknown, g must be estimated, which is the major focus of most PGP approaches. The MCMC approach is generally employed, while the expensive MCMC inference can be avoided by clustering finite differences [15] and input-output pairs [38]. We assume that the region classifier g is already available or can be estimated via one of the aforementioned approaches, thereby focusing more on the estimation of Θ . Since Θ would be inferred by maximizing Equation (4) given D_n , which is generally realized with nonsequential designs, it is unwise to exhaust the sampling budget at the first state. Hence, we take only a small portion in the initial step.

Unfortunately, there is no universal concrete theorem for the optimal portion of initial sampling, while some empirical suggestions can be found in [18], [22]. However, we can conjecture that the number of initial samples has a trade-off property. If the initial sampling is weighed too much, the advantage of active learning will be diluted. Otherwise, active learning can be hindered by low-quality of information come from unreliable intermediate models. Also, when the region

classifier g is not explicitly known so that g must be estimated with the initial samples, the number should be enough to obtain an acceptable g .

B. Partitioned Active Learning Strategy

The essence of active learning is an information criterion function $J : \mathcal{X} \rightarrow \mathcal{R}$ that quantifies the potential importance of a design point in the given set. By optimizing $J(x)$ with respect to $x \in \mathcal{X}$, the next design point is determined and queried to the target function, which is sometimes referred as the oracle in active learning. The variance-based and the IMSE criteria are mostly considered in active learning for GPs due to their versatility and simplicity, so we introduce two criteria and tailor them to establish a new criterion for PGPs.

Suppose we have $D_n \subset \mathcal{X}$, and intend to determine the next location $x_{n+1} \in \mathcal{X}$ with GPs without partitioning. The variance-based criterion is defined as

$$\begin{aligned}J_{\text{VAR}}(x|\Theta_n) &= \sigma_n^2(x) \\ &= k_n(x) - k_n(x, X_n)^\top K_n^{-1} k_n(x, X_n),\end{aligned}\quad (5)$$

where k_n is the kernel function given Θ_n estimated with D_n , and K_n is the covariance matrix comprised of k_n with respect to X_n . The ALM maximizes the variance-based criterion so as to select the location with the greatest predictive uncertainty. The IMSE criterion is calculated by

$$\begin{aligned}J_{\text{IMSE}}(x|\Theta_n) &= \int_{\mathcal{X}} \sigma_{n+1}^2(s|x) ds, \\ \sigma_{n+1}^2(s) &= k_n(s) - k(s, X_{n+1})^\top K_{n+1}^{-1} k(s, X_{n+1}),\end{aligned}\quad (6)$$

where $s \in \mathcal{X}$, $X_{n+1} = (X_n, x)$, and $K_{n+1} = k(X_{n+1})$. Minimizing the IMSE criterion selects the location which is expected to reduce the predictive uncertainty the most over \mathcal{X} , and we refer the active learning with the IMSE criterion as the ALC.

There are more behind derivations of both criteria, while we mention shortly herein. It turns out that the ALM is equivalent to the maximum entropy design, since the choice leads to maximizing the determinant of covariance matrix given Θ_n . Meanwhile, the ALC can be explained with minimizing the generalization error of statistical learning, which can be decomposed to the famous form,

$$\mathbb{E}_{\mathcal{X}}[\|f - H\|^2] = \mathbb{E}_{\mathcal{X}}[\|f - H^*\|^2] + \mathbb{E}_{\mathcal{X}}[\|H^* - H\|^2],$$

where H^* is the best estimation of f in the given PGP class. Assuming the first term representing the bias of the best model is acceptable, the ALC focuses on minimizing the second term, which is the variance. Regarding the variance of H^* as a constant, it becomes minimizing the overall variance of H .

Although the variance-based criterion is more straightforward and numerically inexpensive than the IMSE criterion, the ALC empirically has shown better performance than the ALM [19], [20]. Moreover, one of the promising characteristic of the ALC is that it avoids sampling from the boundary of design space which may provoke loss of information, while the ALM frequently does. It makes the IMSE criterion more appealing to PGPs, since local GPs share common boundaries,

so the variance-based criterion may lead to oversampling near the boundary shared with two adjacent local GPs.

However, the IMSE criterion of (6) does not consider multiple local GPs simultaneously, thus the block diagonal structure of covariance matrix is not involved. Therefore, we dedicate to construction of our criterion for the PGPs by aggregating every information criterion attained by each local GPs. When the IMSE criterion is considered for a candidate location $x \in X_m$ with PGPs, it can be written as

$$J(x|x \in X_{(m)}) = \sum_{i \neq m} \int_{X_{(i)}} \sigma_{(i),n_i}^2(s_{(i)}) ds_{(i)} + \int_{X_{(m)}} \sigma_{(m),n_m+1}^2(s_{(m)}) ds_{(m)}, \quad (7)$$

where $s_{(m)} \in X_{(m)}$ and n_m is the number of samples in X_m . The derivation of (7) is quite straightforward, whereas interpretation of each term therein is worthwhile. The first term is the sum of IMSEs except for $h_{(m)}$, which are invariant to $x \in X_m$. The second term is equivalent to (6), in which $h_{(m)}$ is only considered, so that (7) will only take into account the local region associated with the candidate location. Consequently, there are two main differences in (7): (i) consideration of IMSEs over other local regions; and (ii) the localized IMSE criterion. We focus on each term subsequently considering their meanings, thereby efficiently minimizing (7).

Heuristically, (7) is more likely to be minimized when the most uncertain local GP is taken account into the second term, since the first term can be minimized and the local GP has more potential to be reduced with additional observations. Each IMSE in the first term indicates regional uncertainty of PGP (including $h_{(m)}$'s without additional candidates), thus we can refer to them as global searching prior to considering the second term by using the following criterion

$$J_G(m) = \int_{X_{(m)}} \sigma_{(m),n_m}^2(s_{(m)}) ds_{(m)}, \\ m^* = \arg \max_{m \in \{1, \dots, M\}} J_G(m). \quad (8)$$

A possible problem can be aroused in global searching is that if multiple regions have similar uncertainties, then this scheme will only care about the most uncertain one. However, it can be easily resolved by taking a percentile or providing a threshold to consider multiple regions in the global searching. Once the most uncertain region is determined by (8), we focus on the second term within $X_{(m^*)}$ as local searching, which is

$$J_L(x) = \int_{X_{(m^*)}} \sigma_{(m^*),n_{m^*}+1}^2(s_{(m^*)}|x) ds_{(m^*)}, \\ x^* = \arg \min_{x \in X_{(m^*)}} J_L(x). \quad (9)$$

Since the local GP excludes heterogeneity of other regions that may interrupt approximation of local characteristics, it leads to improvement in exploration by avoiding misleading predictive uncertainty. Therefore, (9) can refer to more relevant information by considering the local GP associated with the region. We call the sequential criteria (8) and (9) by Partitioned IMSE (PIMSE), and the active learning with PIMSE as Partitioned ALC (PALC).

Algorithm 1 PALC

- 1: **Prerequisite:** $M, N_0, N_{Max}, N_{Ref}, N_{Cand}, \mathcal{X}, (D', e^*)$
 - 2: Initialize D with N_0 space-filling design over \mathcal{X}
 - 3: Partition \mathcal{X} into M subregions
 - 4: Fit PGP (H) on D
 - 5: **while** $\text{card}(D) \leq N_{Max}$ and $L_{D'}(H) \geq e^*$ **do**
 - 6: Generate X_{Ref} with N_{Ref} space-filling design over \mathcal{X}
 - 7: Solve $m^* = \arg \max_m J_G(m)$
 - 8: Generate X_{Cand} with N_{Cand} space-filling design over X_{m^*}
 - 9: Solve $x^* = \arg \min_{x \in X_{Cand}} J_L(x)$
 - 10: Observe y^* at x^*
 - 11: $D = D \cup \{(x^*, y^*)\}$
 - 12: Fit $h_{(m)}$ on D
 - 13: **if** D' exists **then**
 - 14: Check $L_{D'}(H) < e^*$
 - 15: **end if**
 - 16: **end while**
-

Two termination criteria are considered in the algorithm. One is based on the time when the iterations reach the pre-defined budget, and the other is the achievement of desired prediction accuracy with the model. The budget criterion is straightforward, while most active learning algorithms may not guarantee that the last model is the best one unless the trained dataset is noise-free. To avoid the unwanted overfitting, early-stopping with a desired prediction accuracy is one possible solution. To utilize the prediction accuracy criterion for the termination, a testing dataset should be stored only for the accuracy evaluation in the learning process.

The pseudocode of PALC is provided in Algorithm 1. In prerequisites, (D', e^*) is optionally required for the predictive accuracy criterion. N_0 and N_{Max} stand for the numbers of initial samples and the maximum attainable samples (i.e., budget) respectively. X_{Ref} is a reference set composed of N_{Ref} space-filling points $(\{s_i\}_{i=1}^{N_{Ref}} \subset \mathcal{X})$, which is needed to implement the global searching approximately as

$$J_G(m) = \frac{1}{N_{Ref}} \sum_{i=1}^{N_{Ref}} \sigma_{(m),n_m}^2(s_i).$$

The subset of X_{Ref} composed of points in $X_{(m^*)}$, which is $\{s_i\}_{i=1}^{N_{Ref}^*}$ will be referred to the local searching subsequently as

$$J_L(x) = \frac{1}{N_{Ref}^*} \sum_{i=1}^{N_{Ref}^*} \sigma_{(m^*),n_{m^*}+1}^2(s_{(m^*),i}|x) ds_{(m^*)}, \quad (10)$$

where $x \in X_{Cand} = \{x_i\}_{i=1}^{N_{Cand}}$. In this paper, we have generated new X_{Ref} and X_{Cand} with LHD in every step in order to encourage exploration.

C. Numerical Remedies for Partitioned Active Learning

The IMSE criterion is numerically more demanding than the variance-based criterion, since it involves the inversion of K_{n+1} which is updated with every candidate. That is,

calculation of the IMSE criterion requires $\mathcal{O}(n^3)$ for each candidate. Moreover, when N candidates are provided to the active learning module, the computational cost is multiplied by the number. Although significance of their effects varies with specific situations, the effect of candidate number can be more considerable than the inversion cost. Therefore, in order to improve the numerical aspect of PALC, we should provide some remedies for both matrix inversion and the number of candidates.

Fortunately, the global searching alleviates the number of candidates by reducing the area of region by taking a smaller region of the design space. Generally, candidates for active learning are given with space-filling or dense-grid over the design space. Both approaches will make the solution of IMSE more close to the global optimum as the number of candidates increases, increasing the cost proportional to the number of candidates. Therefore, it is more promising to generate candidates over a smaller region which is chosen by the global searching. Under this framework, the cost of PIMSE can be reduced proportional to the area of subregion chosen in (8).

The matrix inversion cost of PGP is automatically alleviated by partitioning the design space with the block diagonal covariance matrix. That is, the inversion cost reduces from $\mathcal{O}(n^3)$ to at most $\mathcal{O}(n_m^3)$, where $n_m < n$ usually. Another applicable remedy is updating the inverse of K_{n+1} in (6) exploiting K_n^{-1} iteratively. Although it is possible to apply the Sherman-Morrison formula to get the updated inverse matrix directly as shown in [20], we advocate the Cholesky decomposition for solving the linear system $K_n^{-1}\mathbf{k}$ considering the numerical stability and cost [4]. Given that the Cholesky factor (a lower triangular matrix) of K_n , the Cholesky factor of K_{n+1} with that of K_n . The update only requires a forward substitution step of a size n triangular system, thus it needs only $\mathcal{O}(n_m^2)$ instead of $\mathcal{O}(n_m^3)$. A more detailed procedure of the Cholesky update is provided in Appendix A.

IV. SIMULATION STUDY

In this section, we evaluate our active learning strategy by simulation data. Two functions are considered that can be visualized straightforwardly. These two functions are even and uneven response surfaces. As our benchmark methods, the ALC and the ALM are considered for SGP models, and the variance-based criterion is also applied to PGP models (referred as the PALM).

A. 1-Dimensional Data

We apply our proposed active learning algorithm to a 1-dimensional simulation function

$$f(x) = 2x \sin(8\pi x^3),$$

which is defined on $[0, 1]$ without observation noise as the dotted line in Fig. 2a. We allocate 10 samples for initial training using Maximin LHD, and 20 samples are sequentially obtained via active learning. The RBF kernel is used for GP models. The function is differentiable, with heterogeneous frequency and amplitude over the domain. Although there is no

specific boundary for this function, we rigorously partition the design space with the following translated heaviside function,

$$g(x) = \mathbf{1}_{\{x \geq 0.5\}},$$

which is assumed as the ground truth.

Fig. 2 shows each GP model fitted with initial samples. Fig. 2b presents how the partitioned structure prevent misled active learning by providing appropriate predictive uncertainty. Due to the space-filling property of both variance-based and IMSE criteria, the next query location with the single GP model is chosen within the low frequency region, while the PGP does not. Within the PGP framework, the variance-based criterion takes the point in the boundary, while the IMSE does not, thus the IMSE criterion is more promising.

After full running of each active learning strategies, the learning curves of considered models are presented in Fig. 3. From the result, we can observe that both partitioned active learning strategies outperform the single GP's, and the PALC is slightly better than the PALM. Considering the first query location of each method, it is not so surprising that the PALC is the best. Interestingly, we also notice that PGP's are less accurate than single GPs at the initial state, while PGP's learn much faster than single GPs with the same active learning criteria.

B. 2-Dimensional Data

We expand our active learning experiment on a 2-dimensional function, which is also used in other active learning literature [20], [36]. Since the purpose is to evaluate the performance of the proposed active learning approach, the function is mainly comprised of two regions: even and uneven. In a similar manner, we begin with 15 samples with LHD, and obtain 15 additional samples via active learning.

The function does not allow us an efficient partition with a simple function as the 1-D simulation, we borrow some ideas from [15], exploiting the finite differences between initial samples. Unlikely to their original clustering approach, we use a support vector machine after labeling initial samples based on their magnitudes of finite differences to generate a more flexible boundary than the Voronoi tessellation. Consequently, we obtain a partitioning shown in Fig. 5a. Since region 1 is even, fitting independent GP models induces more relevant importance of design points as shown in Fig. 5c, while the IMSE criterion with a SGP fails to pick within the more interesting region.

TABLE I
TOTAL EXECUTION TIMES OF ACTIVE LEARNING WITH THE IMSE
CRITERION IN THE 2-D SIMULATION STUDY

Strategies	ALC	PALC without Global Search	PALC with Global Search
Time (sec)	45.24	19.81	6.30

Remark. The labeling time is ignored, so times for fitting GP and active learning are considered in the time.

Table I summarizes the results in 2-D simulation study. It turns out that the performance of partitioned active learning

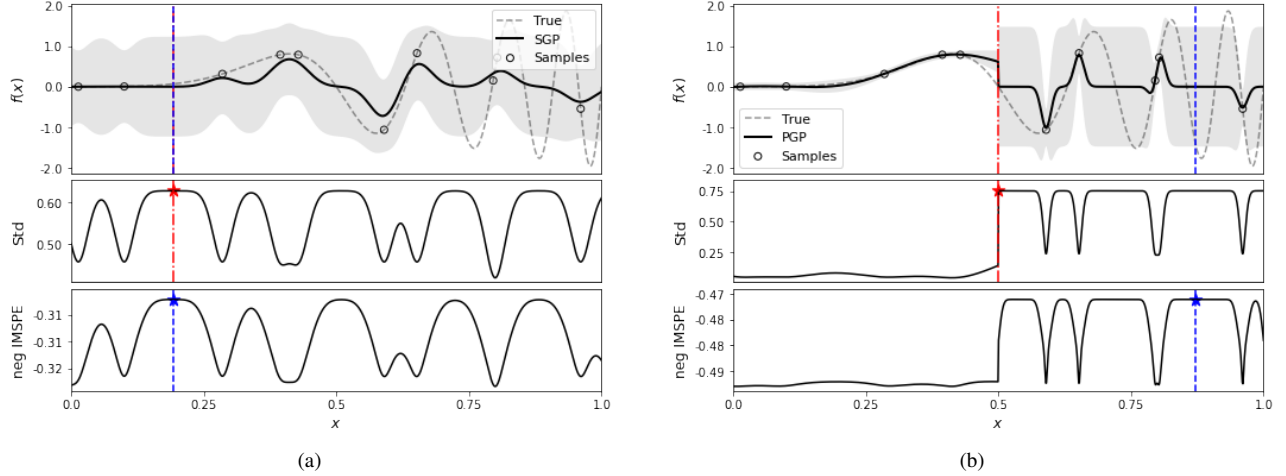


Fig. 2. Fitting GP models on a 1-D simulation function. (a) SGP. (b) PGP with two local GPs. The gray-shaded region indicates 95% predictive interval of each GP model. The PGP is partitioned at $x = 0.5$.

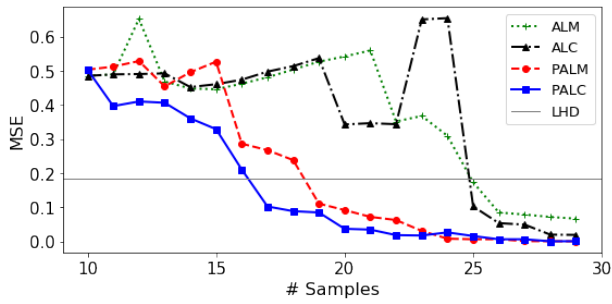


Fig. 3. Learning curves in the 1-D simulation study

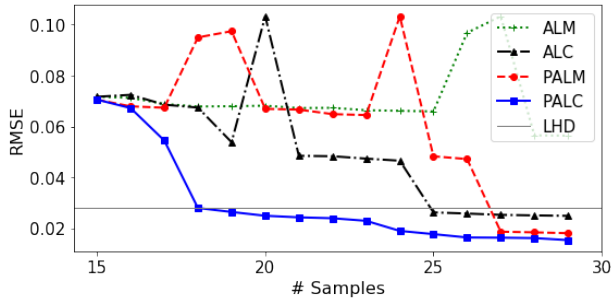


Fig. 4. Learning curves in the 2-D simulation study

surpasses other benchmark methods in this case. Moreover, the global searching shows more consistent progress than the default PALC. It is noteworthy that the global searching procedure reduced the searching time one third of its default ignoring the time of oracle's labeling (19.8 sec \rightarrow 6.5 sec with 1,000 candidate points over the design space). Considering the characteristic of this simulation function, it is more promising to use global skimming when design space is composed of some uninteresting regions.

V. CASE STUDY

In this section, we apply our approach to construct surrogate models for two different real world cases. The original purpose

of surrogate models herein is to embed them into automated systems and to provide uncertainty quantification in posterior analysis. Both case studies include higher dimensional inputs than the previous simulations, and include heterogeneity in their design spaces due to material properties. As our benchmark methods, the SGP with the ALM and the ALC, and the PGP with variance-based criterion (referred as PALM) are commonly considered.

A. Residual Stress of Composite Fuselages

We apply our proposed active learning strategy to the construction of predictive model of residual stress in the composite fuselage assembly process. In the aircraft manufacturing process, composite fuselages are built in several subsections independently, so they are subject to the discrepancy in the junction part. In consequence, the reshaping of composite fuselage is conducted with multiple fixed actuators with the automatic shape control. In order to achieve the optimal manufacturing process, the shape control needs to consider not only the deformation, but also the residual stress of the structure due to their fatal affects on the final product. The development of highly accurate predictive model for the shape control is very challenging, since the problem is endowed with both the heterogeneity and the demanding cost of real experiments. Especially, the stress of composite fuselage is more difficult to predict [10], we apply our method and other benchmarks to the stress predictive modeling.

In order to implement our case study cost-efficiently, we utilized the FEA model, which is well-calibrated based on the real experiment [39]. The simulation mimics the real shape adjustment process that has 10 actuators under the fuselage section as shown in Fig. 6a [40], and the maximum magnitude of actuator's force is 450 lbf. The maximum residual stress on the fuselage section is our interest, which is measured in psi scale. The 10-D design space is partitioned into 3 regions based on the clustering of input and output pairs, and the Matérn kernel is used for each local GPs and SGPs. To observe the effect of global searching in this case, we implemented

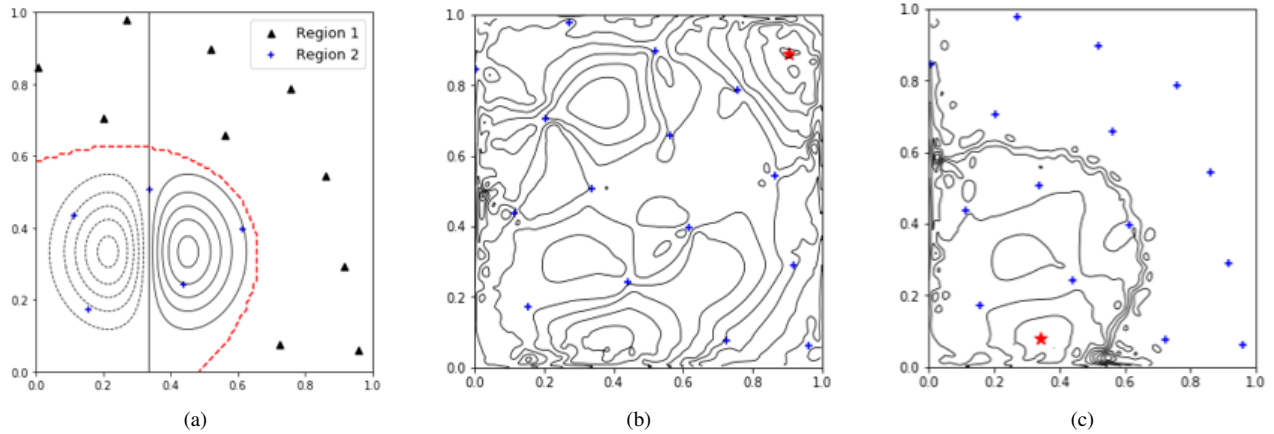


Fig. 5. 2-D simulation study. (a) Initial design points with partitioned regions. (b) IMSE criterion with a single GP. (c) IMSE criterion with a PGP. Blue points represents initial points in (b) and (c), and a red point indicates the chosen location according to each IMSE criterion.

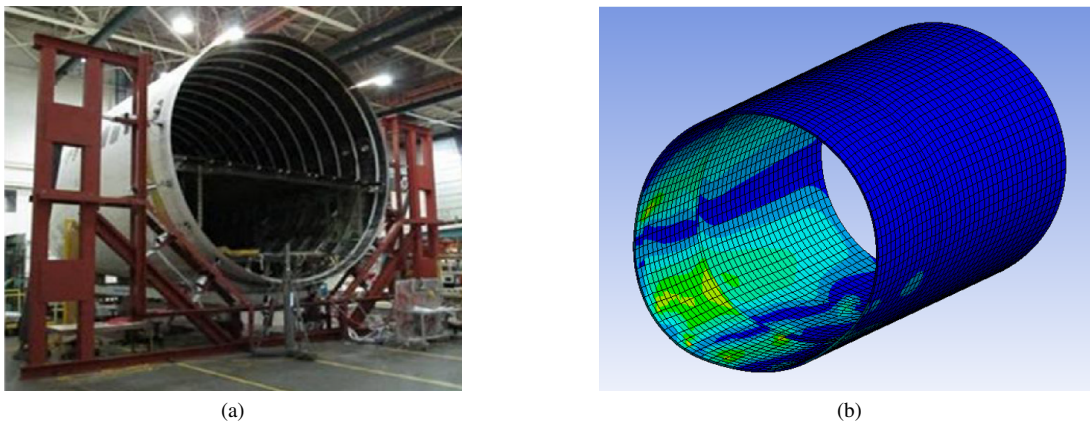


Fig. 6. Shape adjustment of composite fuselage. (a) Composite fuselage installed upon the fixture with actuators. (b) Simulated residual stress of composite fuselage in ANSYS.

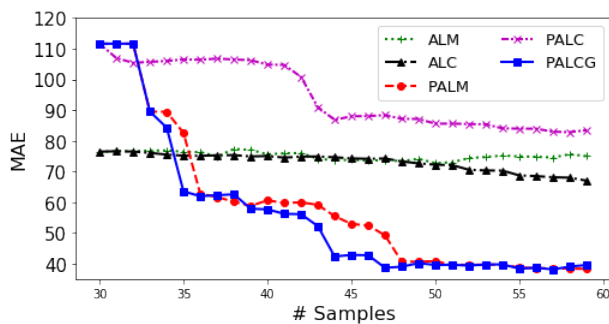


Fig. 7. Learning curves in case study I: Residual stress of composite fuselage.

two types of PALC: (i) without global searching (PALC); and (ii) with global searching (PALCG). As the initial dataset, 30 samples are given with the LHD, and additional 30 samples are sequentially obtained with different active learning strategies. The model evaluation is conducted with a separated testing dataset composed of 100 LHD samples, and mean absolute error (MAE) is used as the metric.

Fig. 7 presents learning curves of considered methods.

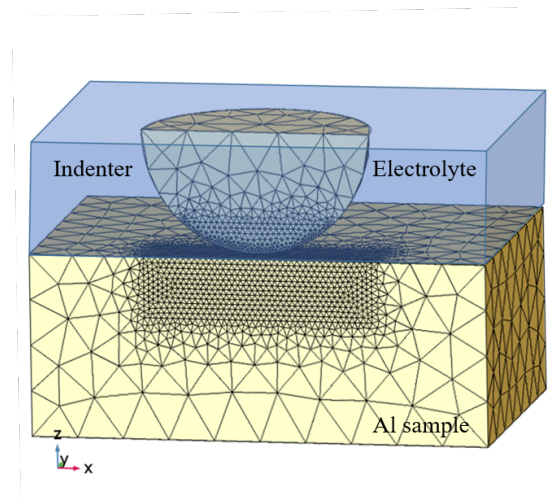


Fig. 8. Schematic tribocorrosion simulation setup.

Interestingly, SGPs with initial dataset outperform PGPs, while they learn less efficiently than them. At the final state, the PALCG and the PALM achieve comparable performance,

surpassing the others. Moreover, the PALC (without global searching) show the worst learning efficiency among all methods. It implies that the global searching scheme does not only alleviates the computational burden by narrowing down the number of candidates, but also improves the efficiency of active learning indeed.

B. Tribocorrosion in Aluminium Alloys

As our second case study, the material loss rate during stress corrosion (i.e. tribocorrosion) in aluminum alloys with 6 control variables are considered. To test the tribocorrosion resistance of metals, experimental tests and FEA simulations were carried out by scratching the surface of the samples in corrosive environment [41], [42] as shown in Fig. 8. During the tribocorrosion process, the mechanical deformation and the electrochemical processes including active corrosion and passivation work synergistically to cause material degradation. The FEA model calculates the contact mechanics between the indenter and the sample and simulate the wear process as well as the wear-accelerated material dissolution of the corrosion process, and generate the volume loss results. The 6 control variables for the FEA model are material property descriptors: young's modulus, yield strength, anodic Tafel slope, anodic exchange current density, cathodic Tafel slope, and cathodic exchange current density. The former two govern the mechanical properties while the latter four determine the corrosion behavior of the alloy. The output of the FEA model is the tribocorrosion rate of the alloy, expressed as volume loss per time.

The surrogate model of the FEA model is constructed to assist the optimal design of alloys with uncertainty quantification and alleviating the high-computational cost of the FEA model. To establish the relationship between material property and tribocorrosion rate, a total of 106 FEA simulations were performed by systematically varying the 6 control variables. Since scales of variables in the dataset are inconsistent, each variable is normalized to be within an unit interval. For evaluation, mean relative error (MRE) is used as the metric due to infinitesimal scale of the output. The MRE is calculated as

$$\text{MRE} = \frac{1}{n} \sum_{i=1}^n \frac{|y_i - H(x_i)|}{|y_i|}.$$

The PGP for this case is composed of 3 local GPs, and the SVC model is used for partitioning based on the normalized input-output pairs. The model training and evaluation is implemented via 5-fold cross-validation. That is, about 84 samples are provided to active learning modules as a candidate set. Each PGP with different active learning strategy is trained up to 40 samples from 5 common initial samples. Fig. 9 shows learning curves of different active learning strategies. Likewise, the initial PGP model is worse than the single GP model, while the PGP model gets better as the active learning proceeds. At the last, we can observe that the PALC outperforms other methods with faster reduction in the testing error.

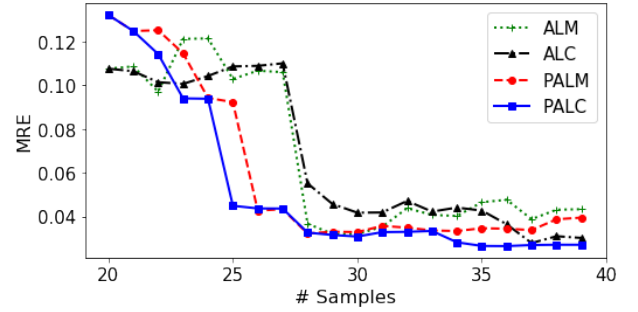


Fig. 9. Learning curves in case study II: Tribocorrosion in aluminum alloys.

VI. CONCLUSION

In order to achieve a reliable and cost-efficient GP modeling for heterogeneous systems, PGP modeling can be served as a promising approach for modeling of the system. However, up to now active learning strategies for GPs have been mostly focused on SGPs that does not benefit PGP modeling. This paper dedicated establishing an efficient partitioned active learning strategy which adopts two-step searching schemes based on the PIMSE criterion structure. By partitioning the design space into multiple subregions according to heterogeneity in the target system, the global searching scheme refers to the integrated predictive uncertainties of local GPs to determine the most uncertain subregion. The global searching scheme allows us to reduce the region of interest, thereby not only accelerating the searching speed, but also improving the overall learning efficiency as shown in the simulation and case studies. The local searching scheme exploited the chosen local GPs in the global searching phase, so the localized IMSE criterion could provide more relevant information minimizing the interruption of other local features in the system.

For the numerical perspective of active learning, applicable numerical solutions are provided: reducing the number of candidates with global searching scheme, and the Cholesky factor update, which can be embedded into the PAL. From two of each simulation and case study, the proposed method outperformed the variance-based criterion, and the SGP with the IMSE criterion. Moreover, the global searching scheme dramatically improved the naive application of IMSE criterion to PGPs in the residual stress of composite fuselage case study. Two successful application of proposed active learning strategy implies that it can be applied to the other domains where the heterogeneity exists.

APPENDIX A

UPDATING CHOLESKY FACTOR FOR PIMSE CRITERION

Suppose we have the Cholesky factor L_n of K_n such that $K_n = L_n L_n^\top$, where L_n can be obtained from fitting the GP with D_n . We aim to get the Cholesky factor L_{n+1} of

$$K_{n+1} = \begin{bmatrix} K_n & \mathbf{k}_n^* \\ \mathbf{k}_n^{*\top} & k_n(x^*) \end{bmatrix},$$

where x^* is a candidate input, and $\mathbf{k}_n = k_n(X_n, x^*)$. Since K_{n+1} shares the same part of K_n , it turns out that $L_{n+1}[:, n, :$

$n]$ is equivalent to L_n . For the rest part (i.e., the last row of L_{n+1}), we can apply the Cholesky-Banachiewicz algorithm as

$$L_{n+1,i} = L_{i,i}^{-1} \left(\mathbf{k}_{n,i}^* - \sum_{k=1}^{i-1} L_{n+1,k} L_{i,k} \right),$$

$$L_{n+1,n+1} = \sqrt{k_n(x^*) - \sum_{k=1}^n L_{n+1,k} \mathbf{v}_k},$$

for $i = 1, \dots, n$.

Rather than calculating the PIMSE directly, the PALC can be faster by skipping redundant computation applying the Cholesky updating approach. The Cholesky factor L_n can be used for the predictive variance of GP in (5) and the global searching criterion of (8) as

$$\sigma_n^2(x) = k_n(x) - \mathbf{k}_n^\top K_n^{-1} \mathbf{k}_n = \mathbf{v}_n^\top \mathbf{v}_n,$$

$$\mathbf{v}_n = L_n \setminus \mathbf{k}_n.$$

In the same manner, the optimal solution of the localized IMSE criterion (9) can be calculated by

$$\sigma_{(m^*), n_{m^*+1}}^2(x) = \mathbf{v}^{*\top} \mathbf{v}^*,$$

$$\mathbf{v}^* = L_{n+1} \setminus k_n(X_{n+1}, x), \quad (11)$$

where $x \in X_{Ref}$ in the case of approximation in (10). Since we already have the solution of (11) partially with \mathbf{v} (i.e., $\mathbf{v}^*[1:n] \equiv \mathbf{v}_n$), we need only $v_{n+1}^* := \mathbf{v}^*[n+1]$, which can be calculated with a forward substitution as

$$v_{n+1}^* = k_n(x_*, x') - \sum_{k=1}^n L_{n+1,k} \mathbf{v}_k.$$

ACKNOWLEDGMENT

We acknowledge the financial support by the US National Science Foundation CMMI-2035038 and CMMI-1855651.

REFERENCES

- [1] M. P. Deisenroth, D. Fox, and C. E. Rasmussen, "Gaussian processes for data-efficient learning in robotics and control," *IEEE Transactions on Pattern Analysis and Machine Intelligence*, vol. 37, no. 2, pp. 408–423, 2013.
- [2] X. Yue, Y. Wen, J. H. Hunt, and J. Shi, "Surrogate model-based control considering uncertainties for composite fuselage assembly," *Journal of Manufacturing Science and Engineering*, vol. 140, no. 4, 2018.
- [3] W. Cho, Y. Kim, and J. Park, "Hierarchical anomaly detection using a multioutput gaussian process," *IEEE Transactions on Automation Science and Engineering*, vol. 17, no. 1, pp. 261–272, 2019.
- [4] C. Rasmussen and C. Williams, *Gaussian Processes for Machine Learning*. Cambridge, MA, USA: MIT Press, Jan. 2006.
- [5] A. T. W. Min, A. Gupta, and Y.-S. Ong, "Generalizing transfer bayesian optimization to source-target heterogeneity," *IEEE Transactions on Automation Science and Engineering*, 2020.
- [6] F. Psarommatis, G. May, P.-A. Dreyfus, and D. Kiritsis, "Zero defect manufacturing: state-of-the-art review, shortcomings and future directions in research," *International Journal of Production Research*, vol. 58, no. 1, pp. 1–17, 2020.
- [7] L. Wright and S. Davidson, "How to tell the difference between a model and a digital twin," *Advanced Modeling and Simulation in Engineering Sciences*, vol. 7, no. 1, pp. 1–13, 2020.
- [8] X. Yue and J. Shi, "Surrogate model-based optimal feed-forward control for dimensional-variation reduction in composite parts' assembly processes," *Journal of Quality Technology*, vol. 50, no. 3, pp. 279–289, 2018.
- [9] M. W. Hyer and S. R. White, *Stress analysis of fiber-reinforced composite materials*. DEStech Publications, Inc, 2009.
- [10] C. Lee, J. Wu, W. Wang, and X. Yue, "Neural network gaussian process considering input uncertainty for composite structures assembly," *IEEE/ASME Transactions on Mechatronics*, 2020.
- [11] T. J. Santner, B. J. Williams, and W. I. Notz, *The design and analysis of computer experiments*. Springer, 2018, vol. 2.
- [12] C. E. Rasmussen and Z. Ghahramani, "Infinite mixtures of gaussian process experts," *Advances in Neural Information Processing Systems*, vol. 2, pp. 881–888, 2002.
- [13] H.-M. Kim, B. K. Mallick, and C. Holmes, "Analyzing nonstationary spatial data using piecewise gaussian processes," *Journal of the American Statistical Association*, vol. 100, no. 470, pp. 653–668, 2005.
- [14] R. B. Gramacy and H. K. H. Lee, "Bayesian treed gaussian process models with an application to computer modeling," *Journal of the American Statistical Association*, vol. 103, no. 483, pp. 1119–1130, 2008.
- [15] M. J. Heaton, W. F. Christensen, and M. A. Terres, "Nonstationary gaussian process models using spatial hierarchical clustering from finite differences," *Technometrics*, vol. 59, no. 1, pp. 93–101, 2017.
- [16] C. A. Pope, J. P. Gosling, S. Barber, J. S. Johnson, T. Yamaguchi, G. Feingold, and P. G. Blackwell, "Gaussian process modeling of heterogeneity and discontinuities using voronoi tessellations," *Technometrics*, pp. 1–20, 2019.
- [17] B. Settles, "Active learning literature survey," University of Wisconsin-Madison Department of Computer Sciences, Tech. Rep., 2009.
- [18] H. Liu, Y.-S. Ong, and J. Cai, "A survey of adaptive sampling for global metamodeling in support of simulation-based complex engineering design," *Structural and Multidisciplinary Optimization*, vol. 57, no. 1, pp. 393–416, 2018.
- [19] S. Seo, M. Wallat, T. Graepel, and K. Obermayer, "Gaussian process regression: Active data selection and test point rejection," in *Mustererkennung 2000*. Springer, 2000, pp. 27–34.
- [20] R. B. Gramacy and H. K. Lee, "Adaptive design and analysis of supercomputer experiments," *Technometrics*, vol. 51, no. 2, pp. 130–145, 2009.
- [21] S. Marmin, D. Ginsbourger, J. Baccou, and J. Liandrat, "Warped gaussian processes and derivative-based sequential designs for functions with heterogeneous variations," *SIAM/ASA Journal on Uncertainty Quantification*, vol. 6, no. 3, pp. 991–1018, 2018.
- [22] X. Yue, Y. Wen, J. H. Hunt, and J. Shi, "Active learning for gaussian process considering uncertainties with application to shape control of composite fuselage," *IEEE Transactions on Automation Science and Engineering*, 2020.
- [23] D. J. MacKay, "Information-based objective functions for active data selection," *Neural Computation*, vol. 4, no. 4, pp. 590–604, 1992.
- [24] D. A. Cohn, Z. Ghahramani, and M. I. Jordan, "Active learning with statistical models," *Journal of Artificial Intelligence Research*, vol. 4, pp. 129–145, 1996.
- [25] E. Uteva, R. S. Graham, R. D. Wilkinson, and R. J. Wheatley, "Active learning in gaussian process interpolation of potential energy surfaces," *The Journal of Chemical Physics*, vol. 149, no. 17, p. 174114, 2018.
- [26] X. Chen and Q. Zhou, "Sequential design strategies for mean response surface metamodeling via stochastic kriging with adaptive exploration and exploitation," *European Journal of Operational Research*, vol. 262, no. 2, pp. 575–585, 2017.
- [27] B. Ankenman, B. L. Nelson, and J. Staum, "Stochastic kriging for simulation metamodeling," *Operations Research*, pp. 371–382, 2010.
- [28] J. Snoek, H. Larochelle, and R. P. Adams, "Practical bayesian optimization of machine learning algorithms," *Advances in Neural Information Processing Systems*, 2012.
- [29] E. Pasolli and F. Melgani, "Gaussian process regression within an active learning scheme," in *2011 IEEE International Geoscience and Remote Sensing Symposium*. IEEE, 2011, pp. 3574–3577.
- [30] A. Freytag, E. Rodner, P. Bodesheim, and J. Denzler, "Labeling examples that matter: Relevance-based active learning with gaussian processes," in *German Conference on Pattern Recognition*. Springer, 2013, pp. 282–291.
- [31] C. Käding, E. Rodner, A. Freytag, O. Mothes, B. Barz, J. Denzler, and C. Z. AG, "Active learning for regression tasks with expected model output changes," in *BMVC*, 2018, p. 103.
- [32] C. B. Erickson, B. E. Ankenman, M. Plumlee, and S. M. Sanchez, "Gradient based criteria for sequential design," in *2018 Winter Simulation Conference (WSC)*. IEEE, 2018, pp. 467–478.
- [33] B. Kim, Y. Lee, and D.-H. Choi, "Construction of the radial basis function based on a sequential sampling approach using cross-validation," *Journal of Mechanical Science and Technology*, vol. 23, no. 12, pp. 3357–3365, 2009.

- [34] M. Heinonen, H. Mannerström, J. Rousu, S. Kaski, and H. Lähdesmäki, “Non-stationary gaussian process regression with hamiltonian monte carlo,” in *Artificial Intelligence and Statistics*. PMLR, 2016, pp. 732–740.
- [35] D. Higdon, “A process-convolution approach to modelling temperatures in the north atlantic ocean,” *Environmental and Ecological Statistics*, vol. 5, no. 2, pp. 173–190, 1998.
- [36] B. Konomi, G. Karagiannis, A. Sarkar, X. Sun, and G. Lin, “Bayesian treed multivariate gaussian process with adaptive design: Application to a carbon capture unit,” *Technometrics*, vol. 56, no. 2, pp. 145–158, 2014.
- [37] C. Cortes, G. DeSalvo, C. Gentile, M. Mohri, and N. Zhang, “Region-based active learning,” in *The 22nd International Conference on Artificial Intelligence and Statistics*. PMLR, 2019, pp. 2801–2809.
- [38] H. T. Nguyen and A. Smeulders, “Active learning using pre-clustering,” in *Proceedings of the Twenty-first International Conference on Machine Learning*, 2004, p. 79.
- [39] Y. Wang, X. Yue, R. Tuo, J. H. Hunt, J. Shi *et al.*, “Effective model calibration via sensible variable identification and adjustment with application to composite fuselage simulation,” *Annals of Applied Statistics*, vol. 14, no. 4, pp. 1759–1776, 2020.
- [40] Y. Wen, X. Yue, J. H. Hunt, and J. Shi, “Feasibility analysis of composite fuselage shape control via finite element analysis,” *Journal of Manufacturing Systems*, vol. 46, pp. 272–281, 2018.
- [41] K. Wang, Y. Wang, X. Yue, and W. Cai, “Multiphysics modeling and uncertainty quantification of tribocorrosion in aluminum alloys,” *Corrosion Science*, vol. 178, p. 109095, 2021.
- [42] K. Wang and W. Cai, “Modeling the effects of individual layer thickness and orientation on the tribocorrosion behavior of al/cu nanostructured metallic multilayers,” *Wear*, p. 203849, 2021.